Supplementary Information for:

Pyridazine-bridged expanded rosarin and semi-rosarinogen

Kui Xu[a], Xiaoshuai Zhang[b], Guopeng Liu[a], Wanzun Ma[a], Yu Yin[a], Ying Yin[b], Xi Chen[a], Lamei Wu[a], Zhengxi Huang[a], Xinyun Zhao*[a], Jonathan L. Sessler*[c], and Zhan Zhang*[a]

[a]Key Laboratory of Catalysis and Energy Materials Chemistry of Ministry of Education & Hubei Key Laboratory of Catalysis and Materials Science, South-Central University for Nationality, Wuhan, Hubei 430074, China

[b]Center for Supramolecular Chemistry and Catalysis, Shanghai University, 99 Shangda Road, Shanghai 200444, China

[c]Department of Chemistry, The University of Texas at Austin, Texas 78712-1224, United States.

Contents

Ⅰ. Synthetic Experimental

General

All reagents and solvents were purchased from commercial suppliers and used without further purification. Analytical thin-layer chromatography (TLC) was performed using commercial pre-coated silica gel plates containing a fluorescent indicator. Column chromatography was carried out using silica gel (0.040-0.063 mm). Mass spectra (MS) were taken on Fisher Orbitrap Elite (ESI), Agilent 6500 quadrupole time-of-flight (Q-TOF) or Bruker (Autoflex speed) matrix-assisted laser desorption ionization time-of-flight mass spectrometric (MALDI-TOF MS) instruments. UV-Vis spectra were recorded on a Varian Cary 5000 spectrophotometer. ^{1}H NMR and ^{13}C NMR spectra were recorded on Bruker AV400 and AV600 instruments. The X-ray crystallographic analysis was carried out on a Brucker D8 instrument. Further details of the structures and their refinement are given in a later section. High performance liquid chromatography (HPLC) was carried out using a CHIRALPAK IA column on a Shimadzu CBM-20A equipped with a UV detector (SPD-M20A).

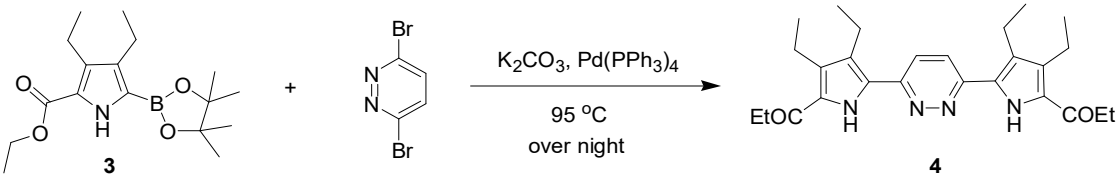

Scheme S1. Synthesis of compound **4**.

Compound 4.[1] Compound **3** was prepared following a reported procedure.[2] A mixture of **3** (3.03 g, 9.45 mmol）, 3,6-dibrobopyridazine (1.06 g, 4.50 mmol), $Pd(PPh_3)_4$ (0.12 g, 0.10 mmol), and K_2CO_3 (6.19 g, 44.81 mmol) was suspended in a solution of 50 mL DMF and 10 mL water under an inert atmosphere. The reaction mixture was heated at 95 °C overnight. After extraction and washing, the product was purified by chromatography over silica gel (ethyl acetate/petroleum ether, 1/5, eluent). After removal of volatiles, compound **4** was obtained as yellow powder (75%). HRMS (ESI, $[M+1]^+$) Calculated for $C_{26}H_{35}N_4O_4$: 467.261. Found: 467.262.

^{1}H NMR (400 MHz, $CDCl_3$) δ = 10.17 (s, 2H), 7.76 (s, 2H), 4.36 (q, *J* = 7.1 Hz, 4H), 2.83 (q, *J* = 7.5 Hz, 4H), 2.77 (q, *J* = 7.5 Hz, 4H), 1.39 (t, *J* = 7.1 Hz, 6H), 1.25 (t, *J* = 7.6 Hz, 6H), 1.20 (t, *J* = 7.5 Hz, 6H).

^{13}C NMR (100 MHz, $CDCl_3$) δ = 160.7, 149.9, 134.6, 127.3, 126.5, 123.1, 120.3, 60.2, 17.9, 17.8, 15.9, 15.6, 14.5.

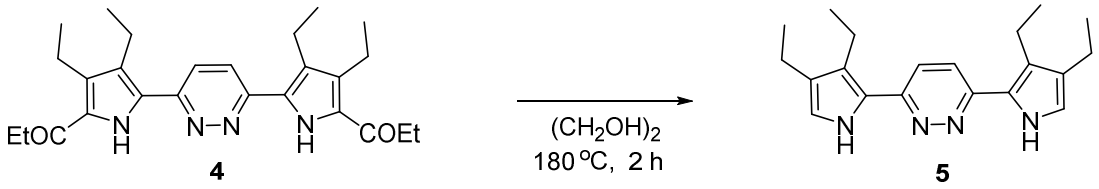

4 5

Scheme S2. Synthesis of compound **5**.

Compound 5.[1] To a round bottom flask containing compound **4** (2.79 g, 6.42 mmol) was charged 20 mL ethylene glycol under an inert atmosphere. After the mixture was heated at 180 ℃ for two hours, the solution was allowed to cool and then further chilled. The product was collected by filtration (96%). HRMS (ESI, $[M+1]^+$) Calculated for $C_{20}H_{27}N_4$: 323.219. Found: 323.220.

^{1}H NMR (400 MHz, $CDCl_3$) δ = 9.60 (s, 1H), 7.63 (s, 1H), 6.74 (d, *J* = 2.6 Hz, 1H), 2.75 (q, *J* = 7.5 Hz, 2H), 2.52 (q, *J* = 7.5 Hz, 2H), 1.25 (m, *J* = 7.5, 2.9 Hz, 6H).

^{13}C NMR (100 MHz, $CDCl_3$) δ = 149.9, 127.1, 125.5, 123.9, 122.2, 117.3, 18.3, 18.1, 15.4, 14.9.

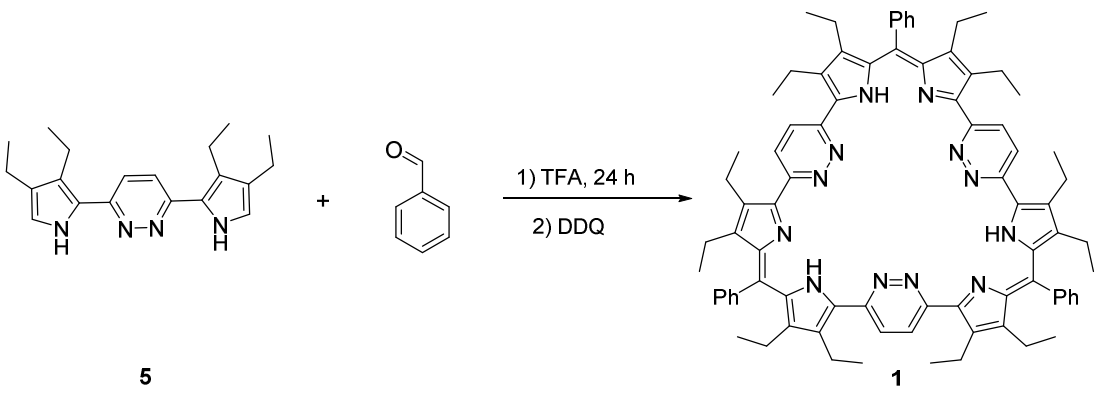

5 1

Scheme S3. Synthesis of **1**.

Expanded rosarin 1. Compound **5** (0.32 g, 1.01 mmol) and benzaldehyde (0.11 g, 1.06 mmol) were placed in a round bottom flask to which was added 20 mL TFA. After stirring for 5 min, the mixture was allowed to react at 60 ℃ for 24 h. After allowing to cool to rt, DDQ (0.23 g, 1.00 mmol) in dichloromethane (DCM) was added to the reaction vessel. The mixture was kept at rt for another 3 h before being poured into chilled water. The resulting mixture was then extracted with DCM and washed with an aqueous solution of K_2CO_3. The product was purified by chromatography over silica gel (ethyl acetate/petroleum ether, 1/5, eluent). Yield: 12%. HRMS (ESI, $[M+1]^+$) Calculated for $C_{81}H_{85}N_{12}$: 1225.697. Found: 1229.696.

^{1}H NMR (400 MHz, $CDCl_3$) δ = 12.06 (s, 3H), 8.06 (s, 6H), 7.54 – 7.41 (m, 16H), 2.82 (q, *J* = 7.4 Hz, 12H), 1.75 (q, *J* = 7.4 Hz, 12H), 1.07 (t, *J* = 7.4 Hz, 18H), 0.72 (t, *J* = 7.4 Hz, 18H).

^{13}C NMR (100 MHz, $CDCl_3$) δ = 153.8, 148.6, 142.5, 142.3, 140.6, 137.8, 136.0, 131.0, 129.4, 127.9, 124.7, 100.0, 31.9, 31.4, 30.2, 29.7, 29.6, 22.7, 18.4, 18.3, 16.4, 15.4, 15.4, 14.1.

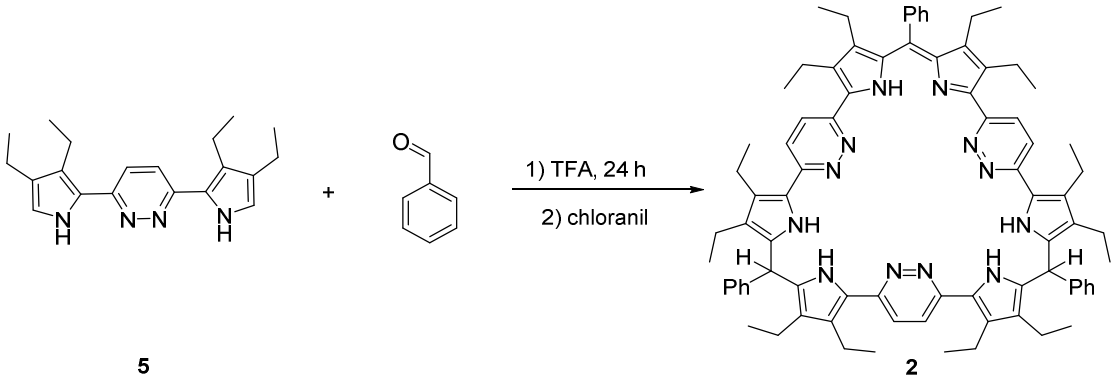

5 **2**

Scheme S4. Synthesis of compound **2**.

Expanded semi-rosarinogen 2. Macrocycle **2** was prepared following the synthetic procedure of **1** except that chloranil instead of DDQ was used as the oxidant. The product was purified as the main fraction by column chromatography over silica gel (ethyl acetate/petroleum ether, 1/5, eluent). Yield: 30%. HRMS (ESI, $[M+1]^+$) Calculated for $C_{81}H_{89}N_{12}$: 1229.728. Found: 1229.724.

^{1}H NMR (400 MHz, DCM-d_2) δ 12.14 (s, 1H), 9.13 (s, 2H), 8.70 (s, 2H), 7.87 (d, *J* = 9.1 Hz, 2H), 7.63 – 7.59 (m, 3H), 7.58-7.54 (m, 4H), 7.51 (d, *J* = 7.2 Hz, 2H), 7.42 – 7.36 (m, 4H), 7.32 (t, *J* = 7.6, 5.3 Hz, 6H), 5.76 (s, 2H), 2.89 (m, *J* = 7.3 Hz, 6H), 2.77 (m, *J* = 7.7 Hz, 6H), 2.56 – 2.39 (m, 8H), 1.91 – 1.79 (m, 2H), 1.73 (m, *J* = 6.9 Hz, 2H), 1.27 (t, *J* = 7.4 Hz, 13H), 1.18 (t, *J* = 7.4 Hz, 6H), 1.01 (m, *J* = 18.7 Hz, 12H), 0.77 (t, *J* = 7.4 Hz, 6H).

^{13}C NMR (100 MHz, DCM-d_2) δ 152.0, 151.6, 149.4, 148.3, 142.5, 141.4, 140.6, 139.7, 137.7, 134.7, 130.8, 130.8, 129.9, 129.5, 128.9, 127.8, 127.2, 126.5, 124.9, 124.5, 123.5, 123.1, 122.6, 122.0, 121.8, 60.2, 40.5, 18.4, 18.2, 17.2, 17.1, 16.4, 15.7, 15.5, 15.4, 15.3.

Ⅱ. NMR Spectral Studies

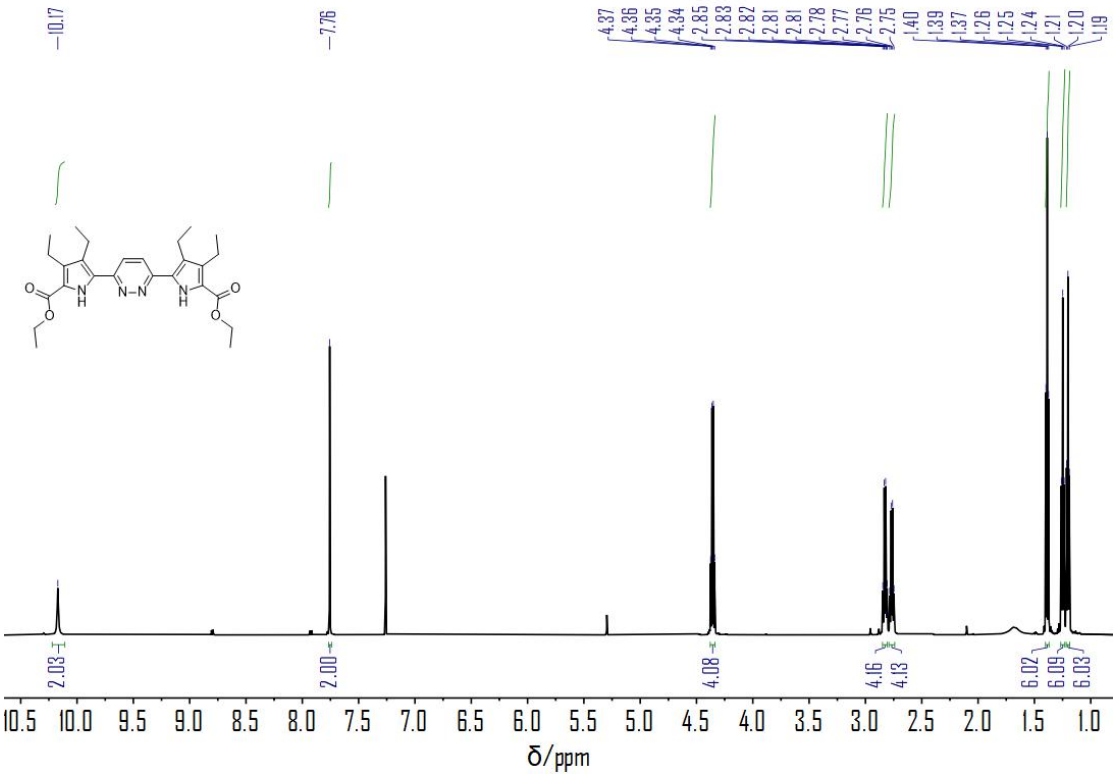

Figure S1. ^{1}H NMR spectrum of **4** recorded in $CDCl_3$ at rt.

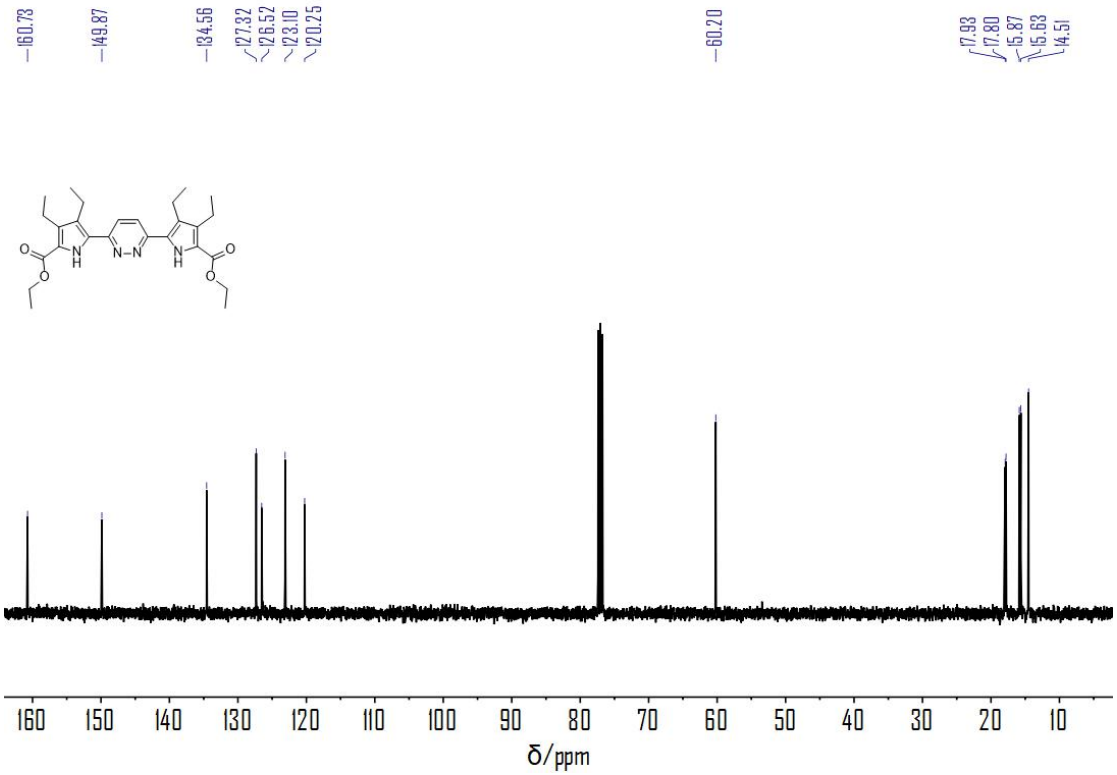

Figure S2. ^{13}C NMR spectrum of **4** recorded in $CDCl_3$ at rt.

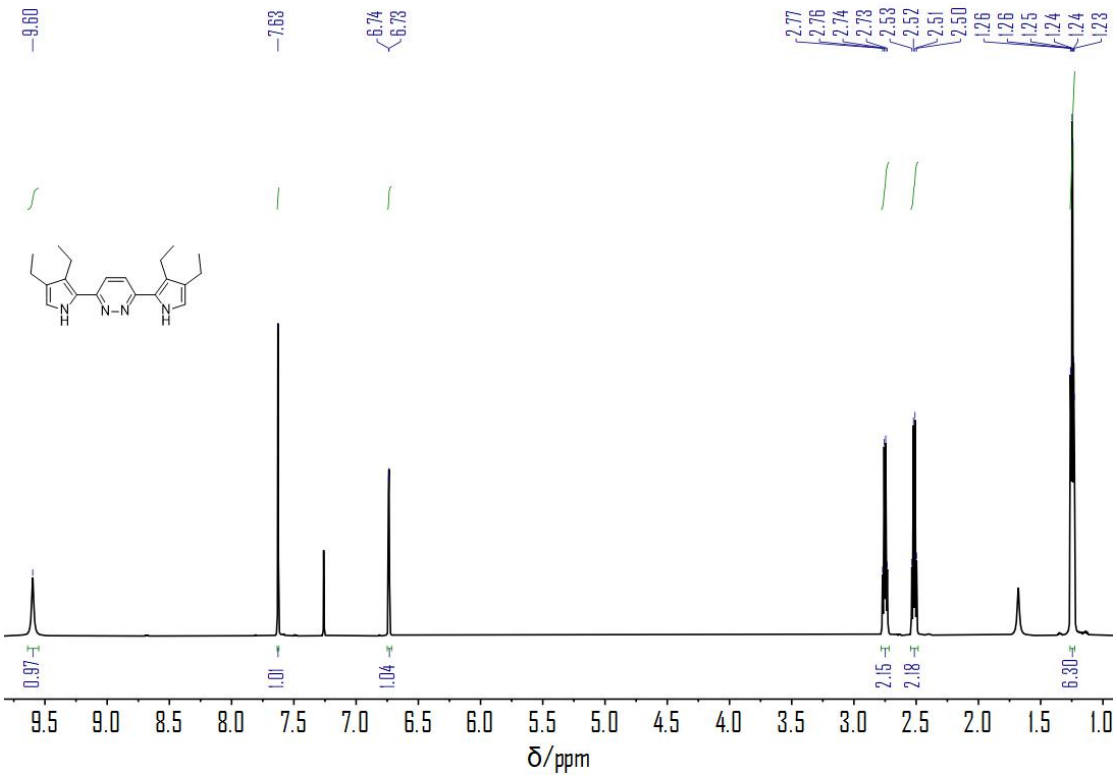

Figure S3. ^{1}H NMR spectrum of **5** recorded in $CDCl_3$ at rt.

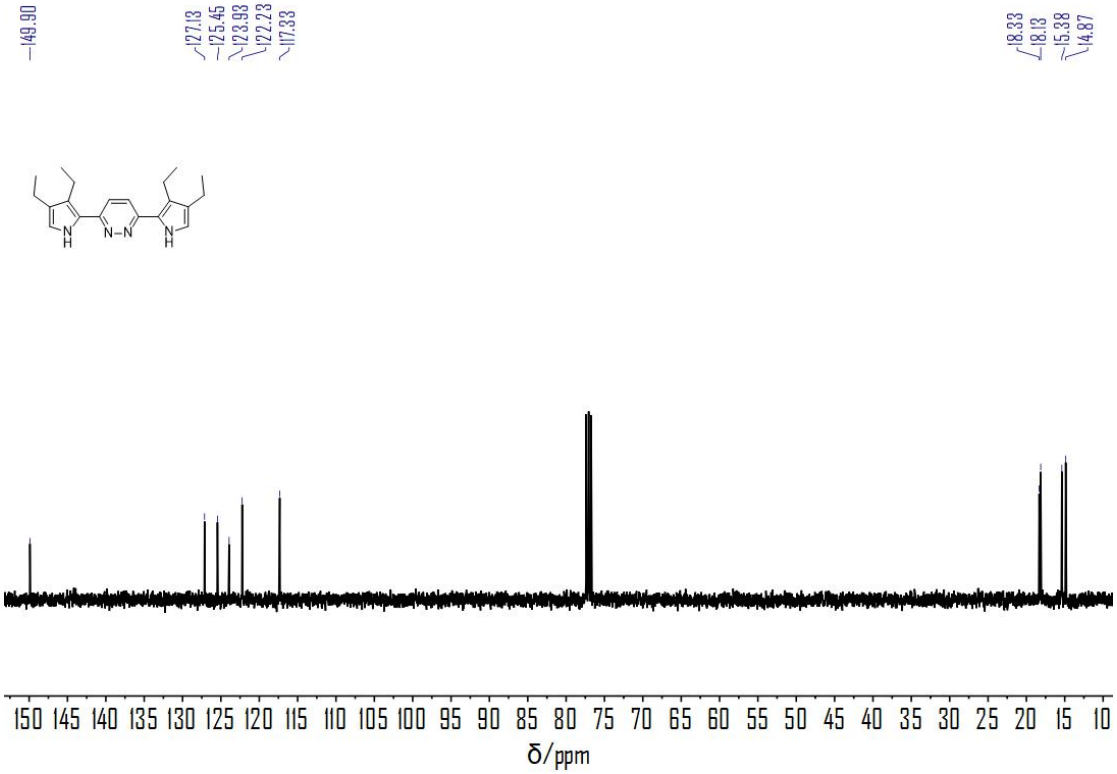

Figure S4. ^{13}C NMR spectrum of **5** recorded in $CDCl_3$ at rt.

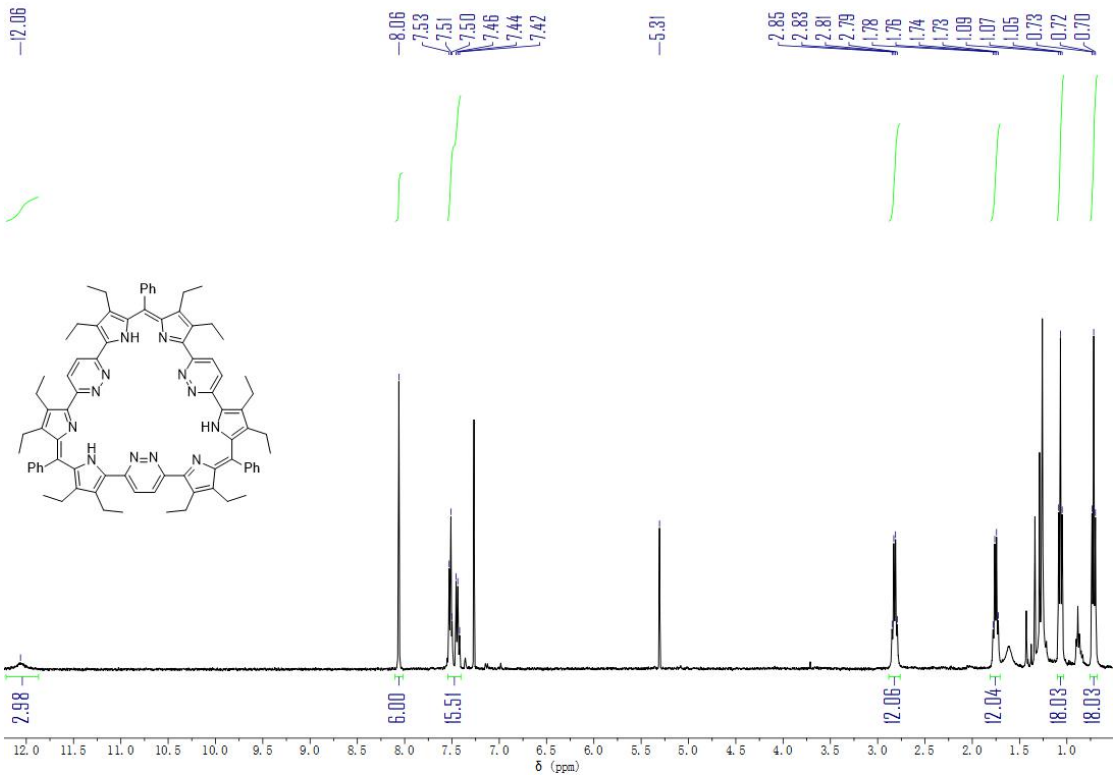

Figure S5. ^{1}H NMR spectrum of **1** recorded in $CDCl_3$ at rt.

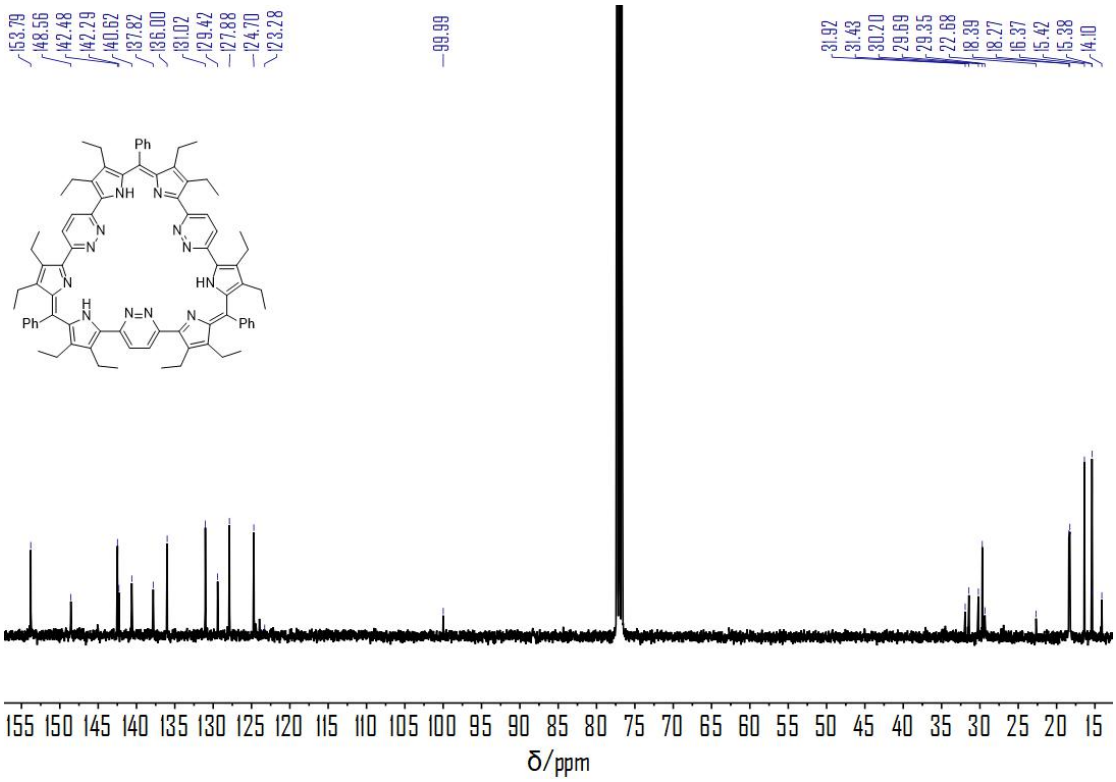

Figure S6. ^{13}C NMR spectrum of **1** recorded in $CDCl_3$ at rt.

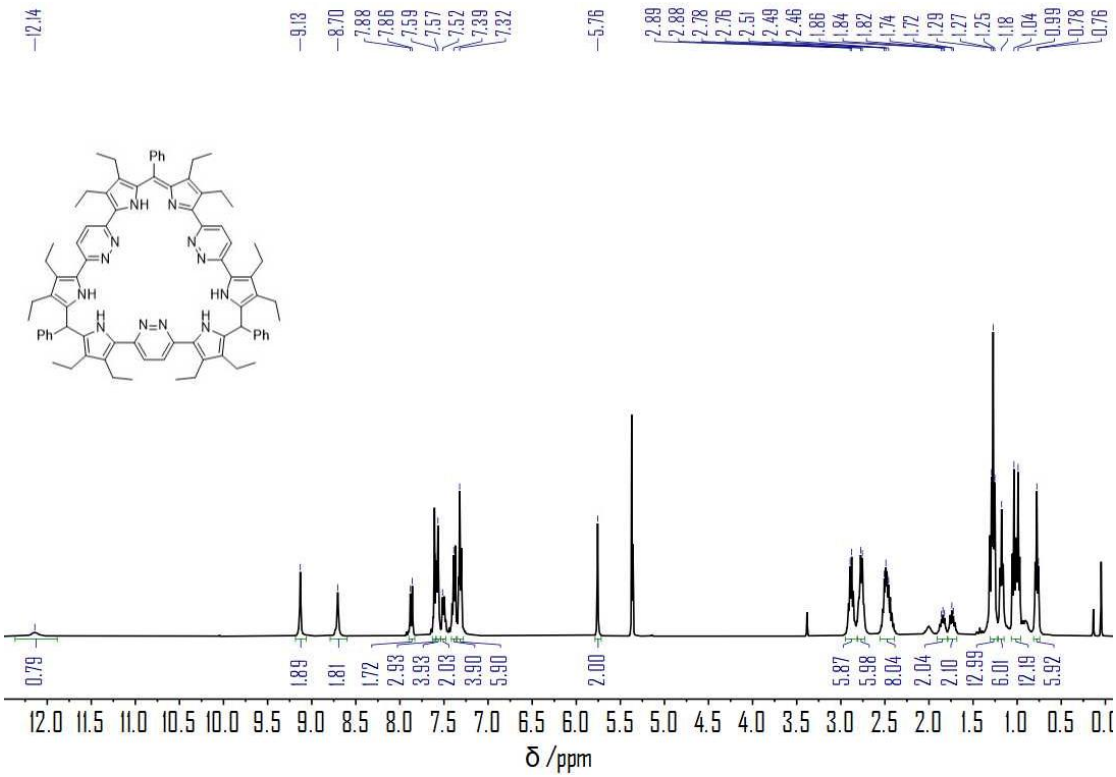

Figure S7. ^{1}H NMR spectrum of **2** recorded in CD_2Cl_2 at rt.

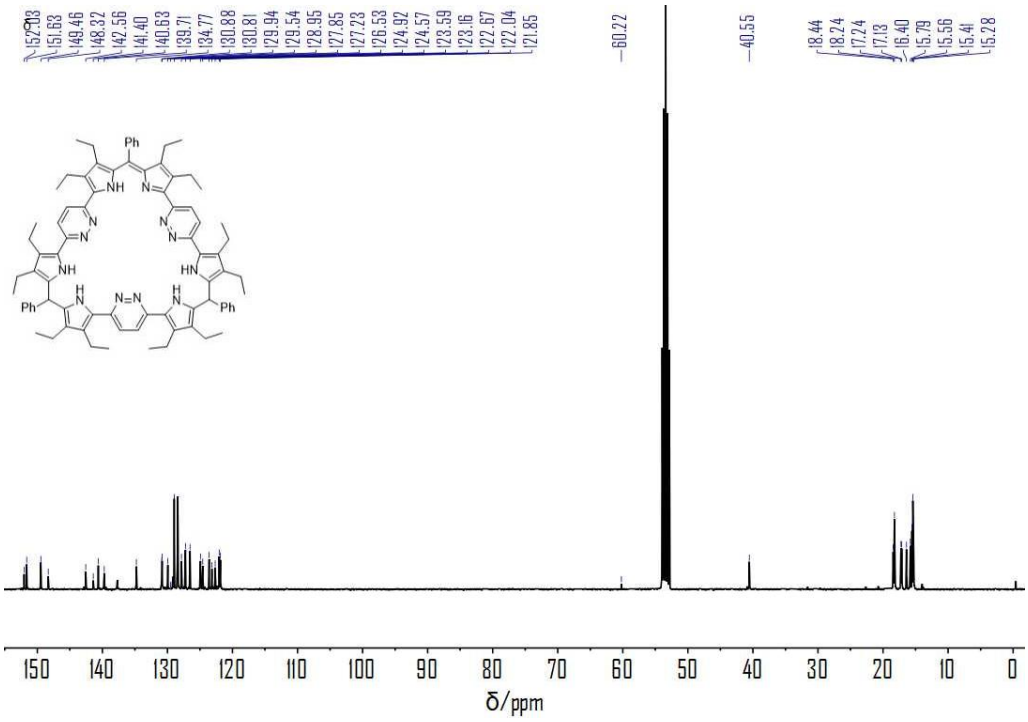

Figure S8. ^{13}C NMR spectrum of **2** recorded in CD_2Cl_2 at rt.

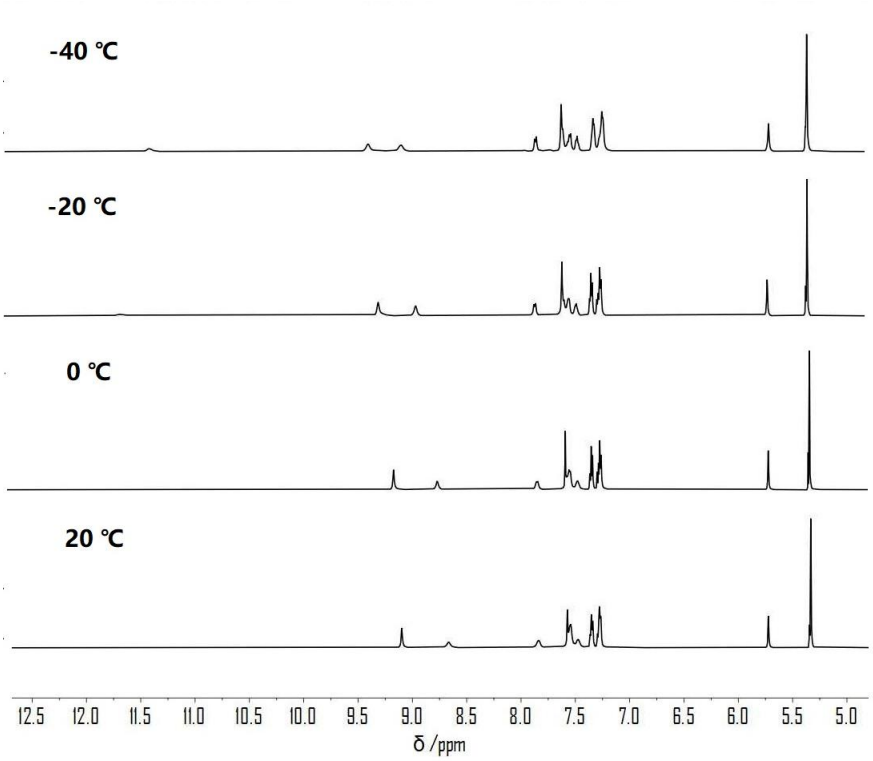

Figure S9. Various-temperature NMR spectra of **2** recorded in CD_2Cl_2.

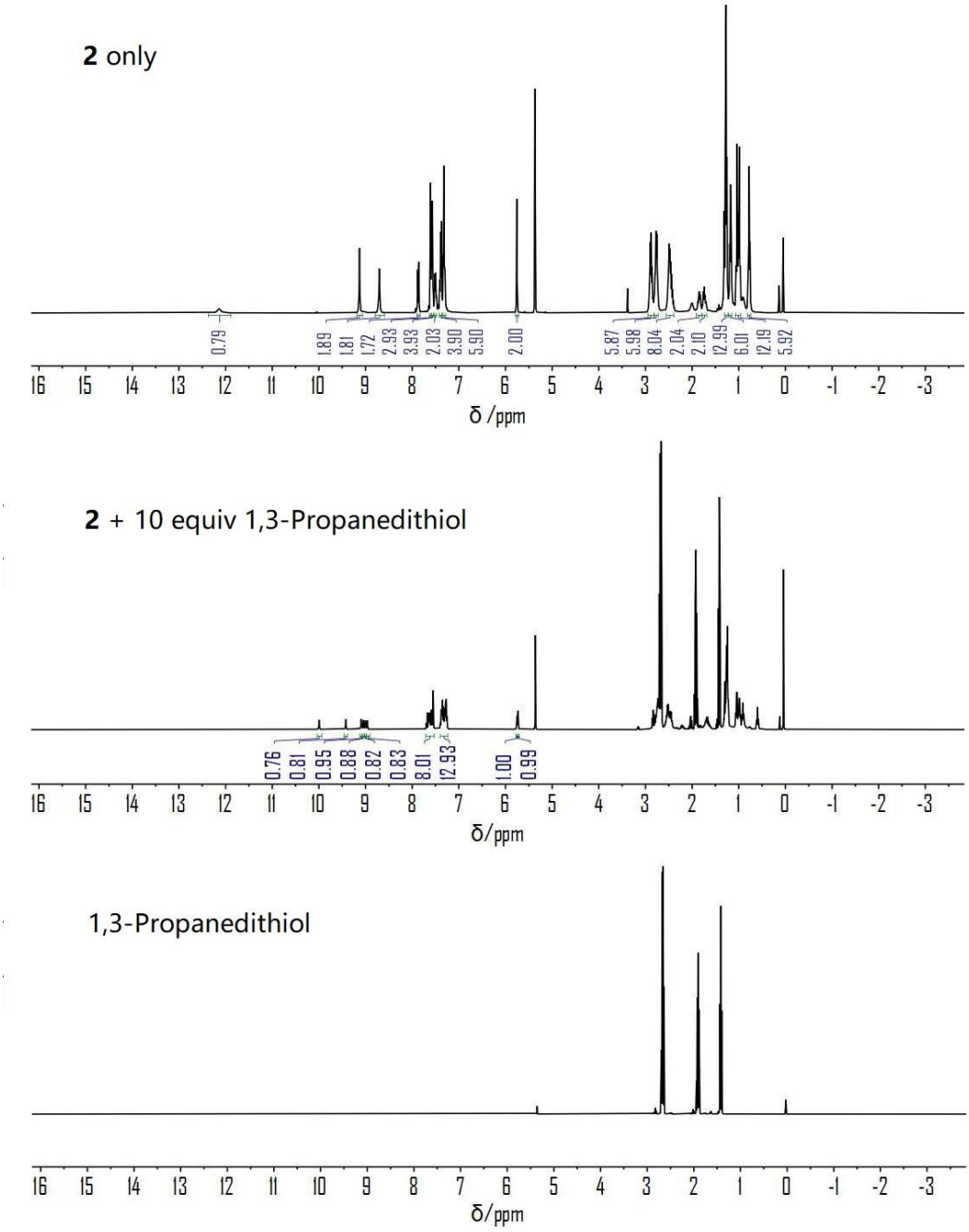

Figure S10. ^{1}H NMR spectra of **2**, 1,3-propanedithiol, and the reaction mixture of **2** and 10 equivalents of 1,3-propanedithiol. The spectra were recorded in CD_2Cl_2 at rt.

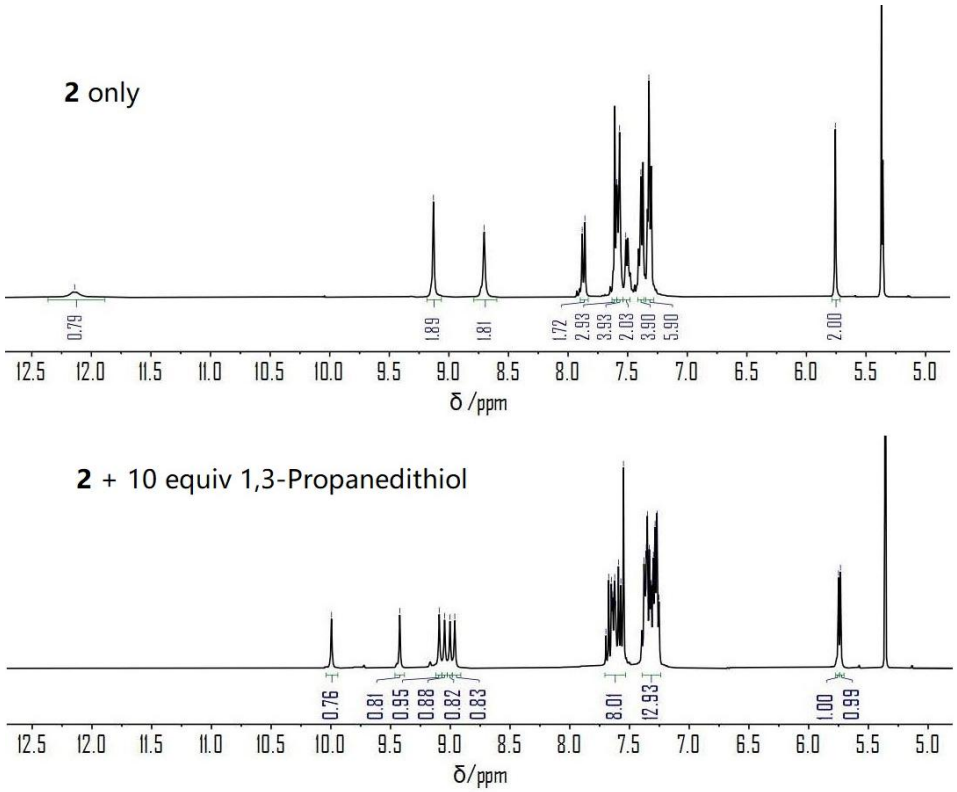

Figure S11. Partial ^{1}H NMR spectra of **2** and the reaction mixture of **2** and 1,3-propanedithiol recorded in CD_2Cl_2 at rt.

Ⅲ. UV-Vis Spectral Studies

Table S1: Colour changes (λ_{max}) seen when **1** is treated with various thiols (in excess).

A: *p*-Toluenethiol; **B**: 4-Aminothiophenol; **C**: 4-Nitrothiophenol; **D**: 1,2-Ethanedithiol; **E**: 1,3-Propanedithiol; **F**: 2-Hydroxy-1-ethanethiol; **G**: 1-Propanethiol; **H**: 1-Butanethiol; **I**: 2-Methyl-2-propanethiol; **J**: 1-Octadecanethiol.

		A	**B**	**C**	**D**	**E**	**F**	**G**	**H**	**I**	**J**
Chloroform	0 h	Pale (553 nm)	yellow[#] (560 nm)	*	dark purple (404 nm, 549 nm	light blue (581 nm, 635 nm)	Grey (broad bands)	×	×	×	×
	6 h				light blue (577 nm)			Grey (551 nm, 605 nm)	Grey (554 nm, 610 nm)	×	×
	12 h							Grey (broad bands)	light blue (618 nm)	×	dark purple (401 nm, 549 nm)
THF	0 h	dark purple (546 nm)	yellow[#] (549 nm)	no reaction[$]	×	dark purple (558 nm, 610 nm)	×	×	×	×	×
	6 h				dark purple (546 nm, 604 nm)	light blue (575 nm, 613 nm)	×	×	×	×	×
	12 h				Grey (571 nm, 607 nm)		Grey (548 nm, 613 nm)	dark purple (544 nm, 607 nm)	dark purple (544 nm, 607 nm)	×	dark purple (544 nm, 607 nm)

	20 h				light blue (572 nm, 608 nm)		light blue (576 nm, 614 nm)	Grey (545 nm, 610 nm)	Grey (546 nm, 610 nm)	×	Grey (546 nm, 610 nm)
DMSO	0 h	Grey (551 nm, 619 nm)	yellow[#] (552 nm)	no reaction[$]	Grey (557 nm, 614 nm)	×	Pale (broad bands)	×	×	×	*
	6 h				light blue (broad bands)	Pale (552 nm, 615 nm)	light blue (589 nm, 627 nm)	Grey (548 nm)	Grey (548 nm)	×	
	12 h							Grey (550 nm)	Grey (549 nm)	×	

[#] Colour reflects contributions from the putative reaction products and excess 4-aminothiophenol (yellow). * Not tested due to poor solubility. [$] The only discernible colour is ascribed to the presence of excess 4-nitrothiophenol (yellow). × No discernible colour change is seen. Note: Blank cells in the table mean that there was NO FURTHER colour change after the initial colour change.

Table S2: Colour changes (λ_{max}) seen when **2** is treated with various thiols (in excess).

A: p-Toluenethiol; **B**: 4-Aminothiophenol; **C**: 4-Nitrothiophenol; **D**: 1,2-Ethanedithiol; **E**: 1,3-Propanedithiol; **F**: 2-Hydroxy-1-ethanethiol; **G**: 1-Propanethiol; **H**: 1-Butanethiol; **I**: 2-Methyl-2-propanethiol.

		A	**B**	**C**	**D**	**E**	**F**	**G**	**H**	**I**
Chloroform	0 h	Pale (546 nm)	yellow[#] (545 nm)	*	Pale (546 nm)	Grey (broad bands)	Pale (550 nm)	slight loss of colour	slight loss of colour	×
	2 h							Pale (537 nm, 683 nm)	Pale (546 nm, 687 nm)	×
THF	0 h	Pale (557 nm)	yellow[#] (557 nm)	no reaction[$]	Pale (555 nm)	Pale (555 nm)	Pale (555 nm)	slight loss of colour	slight loss of colour	×
	6 h							Grey (573 nm)	Pale (557 nm)	×
DMSO	0 h	Blue (561 nm, 684 nm)	yellow[#] (568 nm)	no reaction[$]	Pale (broad bands)	Pale (493 nm)	Pale (571 nm)	slight loss of colour	slight loss of colour	×
	4 h							Pale (571 nm)	Pale (573 nm)	×

[#] Colour reflects contributions from the putative reaction products and excess 4-aminothiophenol (yellow). * Not tested due to poor solubility. [$] The only discernible colour is ascribed to the presence of excess 4-nitrothiophenol (yellow). × No discernible colour change is seen. Note: Blank cells in the table mean that there was NO FURTHER colour change after the initial colour change.

Note: If not otherwise indicated, the sample concentration of **1** and **2** is 3.0 × 10^{-5} mol/L in the solutions used for the photographic studies. The samples were further diluted for the UV-Vis studies.

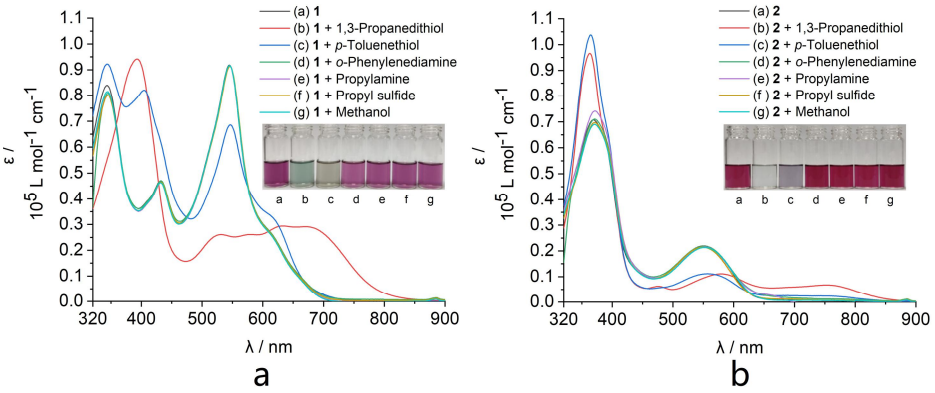

Figure S12. UV-Vis absorption spectra and photos of **1** (a) and **2** (b) in $CHCl_3$ as recorded upon the addition of thiols, amines, sulfide or methanol.

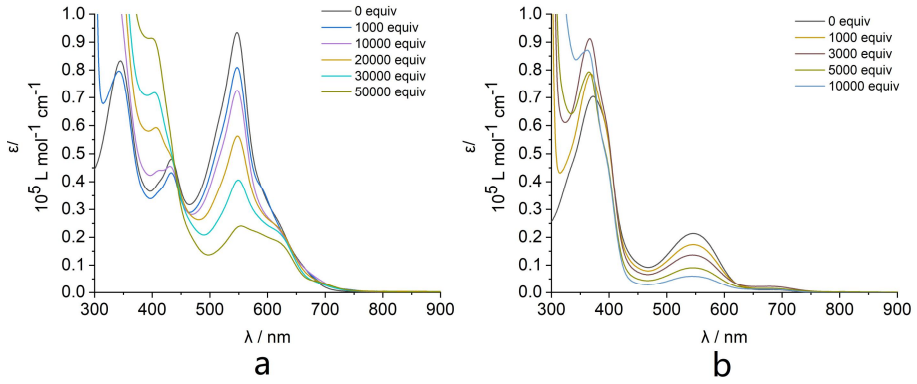

Figure S13. UV-Vis absorption spectra of **1** (a) and **2** (b) recorded after treatment with increasing quantities of *p*-toluenethiol in $CHCl_3$.

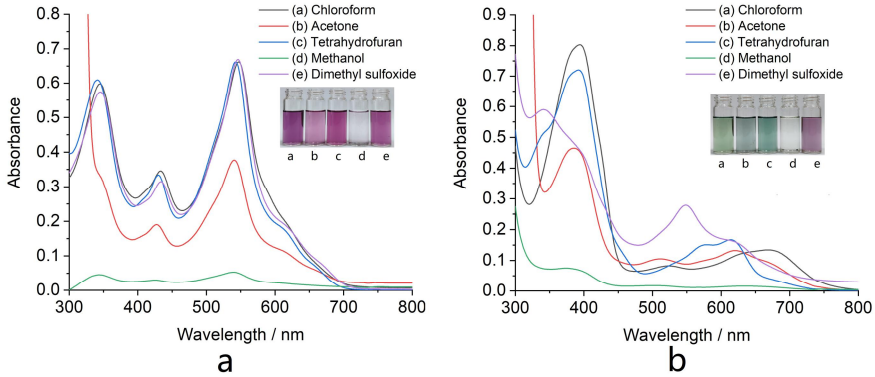

Figure S14. UV-Vis absorption spectra and photos of **1** in different solvents before (a) and after addition of 1,3-propanedithiol (b). Note: **1** did not dissolve in methanol.

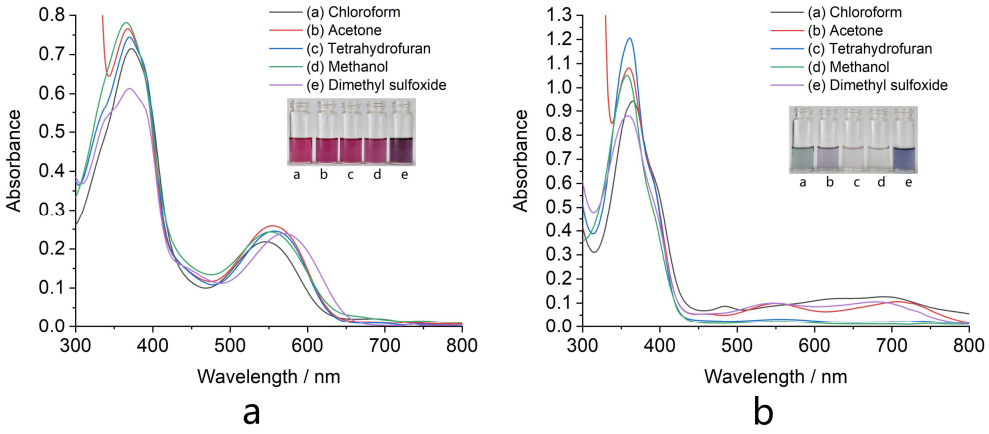

Figure S15. UV-Vis absorption spectra and photos of **2** in different solvents before (a) and after addition of 1,3-propanedithiol (b).

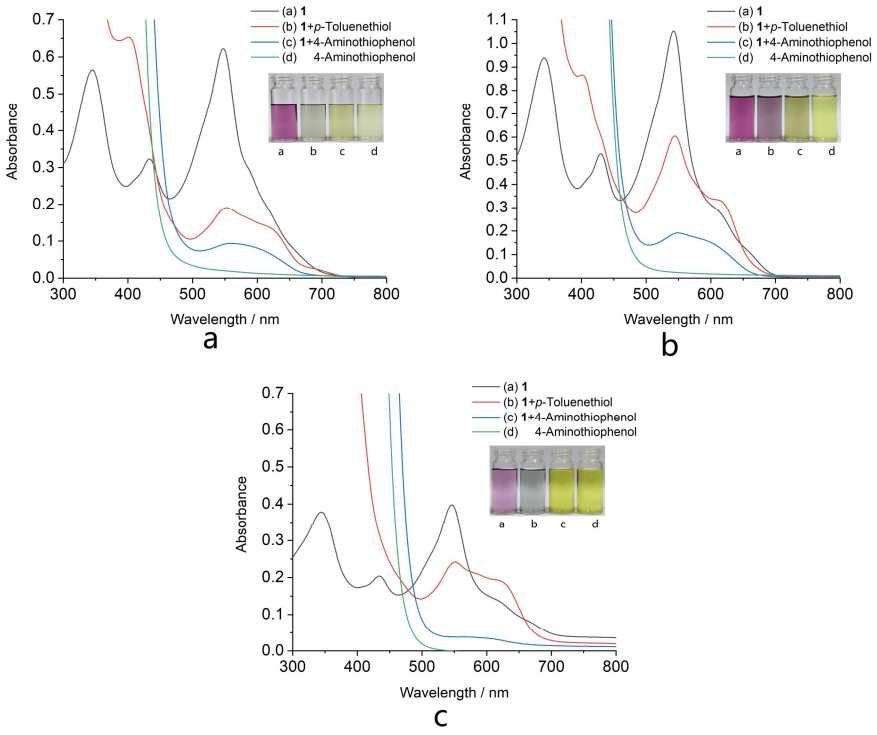

Figure S16. UV-Vis absorption spectra and photos of **1** in chloroform (a), THF (b) and DMSO (c) after the addition of the indicated thiophenol. The concentration of **1** in DMSO is 5.0×10^{-6} mol/L.

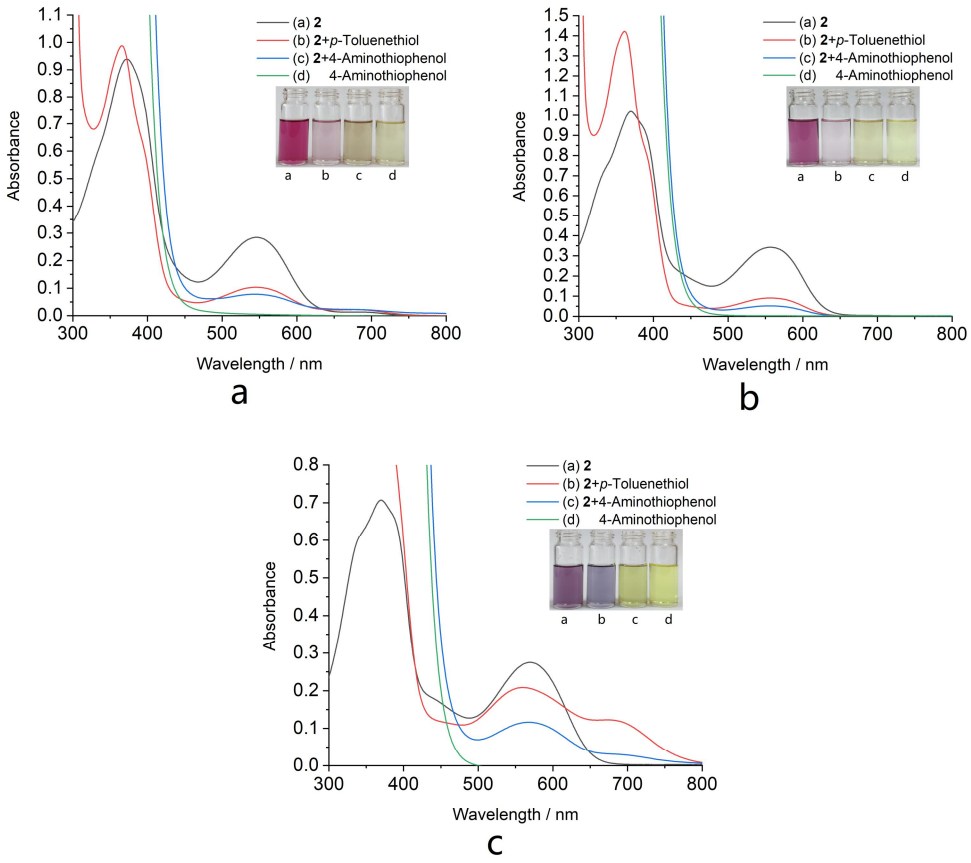

Figure S17. UV-Vis absorption spectra and photos of **2** in chloroform (a), THF (b) and DMSO (c) upon the addition of the indicated thiophenol.

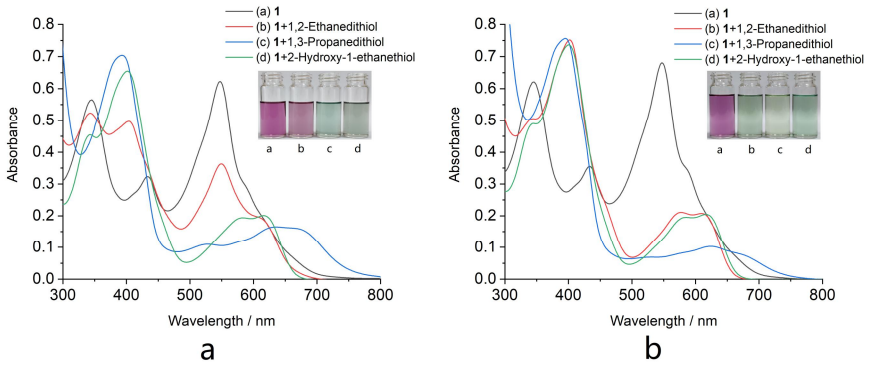

Figure S18. UV-Vis absorption spectra and photos of **1** in chloroform after the addition of a dithiol or 2-hydroxy-1-ethanethiol. (a): Immediately after the addition; (b): 6 h later.

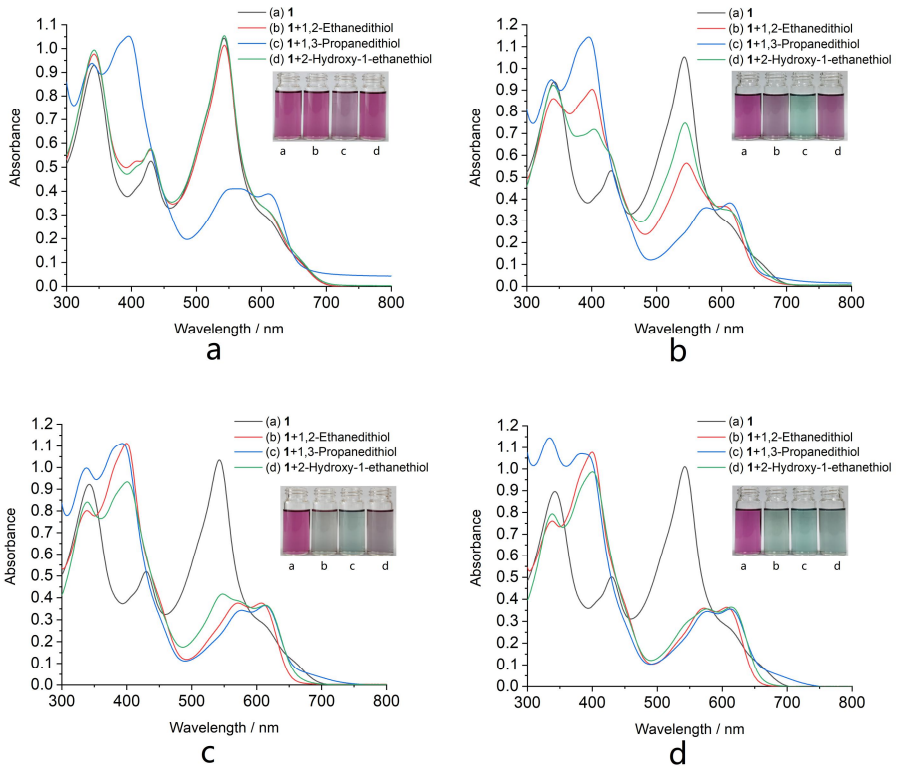

Figure S19. UV-Vis absorption spectra and photos of **1** in THF after the addition of a dithiol or 2-hydroxy-1-ethanethiol. (a): Immediately after the addition and after (b): 6 h; (c): 12 h; (d): 20 h.

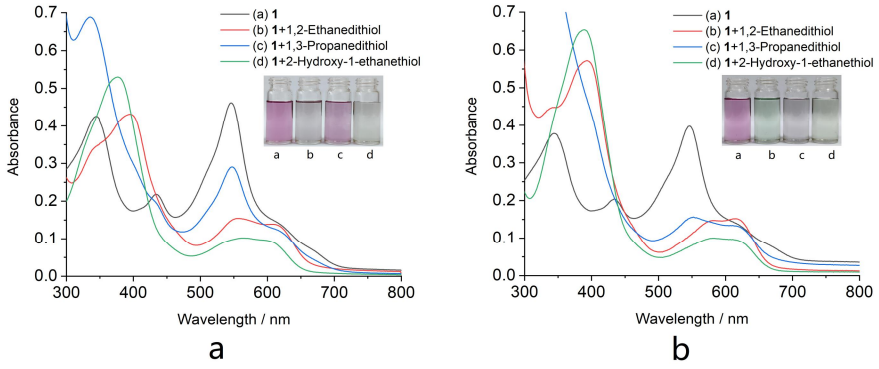

Figure S20. UV-Vis absorption spectra and photos of **1** in DMSO after the addition of a dithiol or 2-hydroxy-1-ethanethiol. (a): Immediately after the addition; (b): 6 h later. The concentration of **1** is 5.0×10^{-6} mol/L.

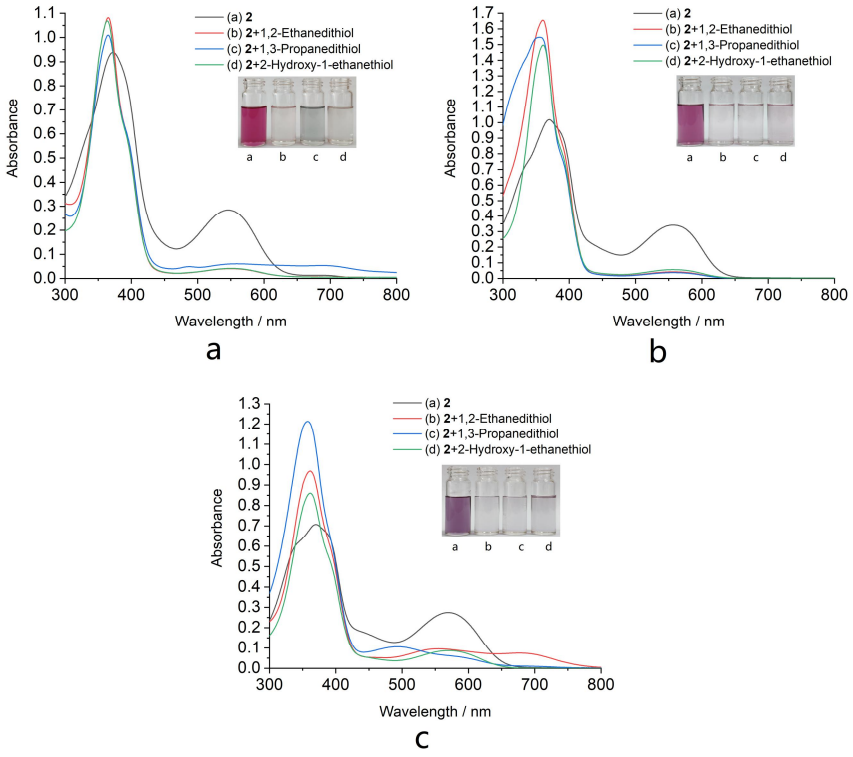

Figure S21. UV-Vis absorption spectra and photos of **2** in chloroform (a), THF (b) and DMSO (c) upon the addition of a dithiol or 2-hydroxy-1-ethanethiol.

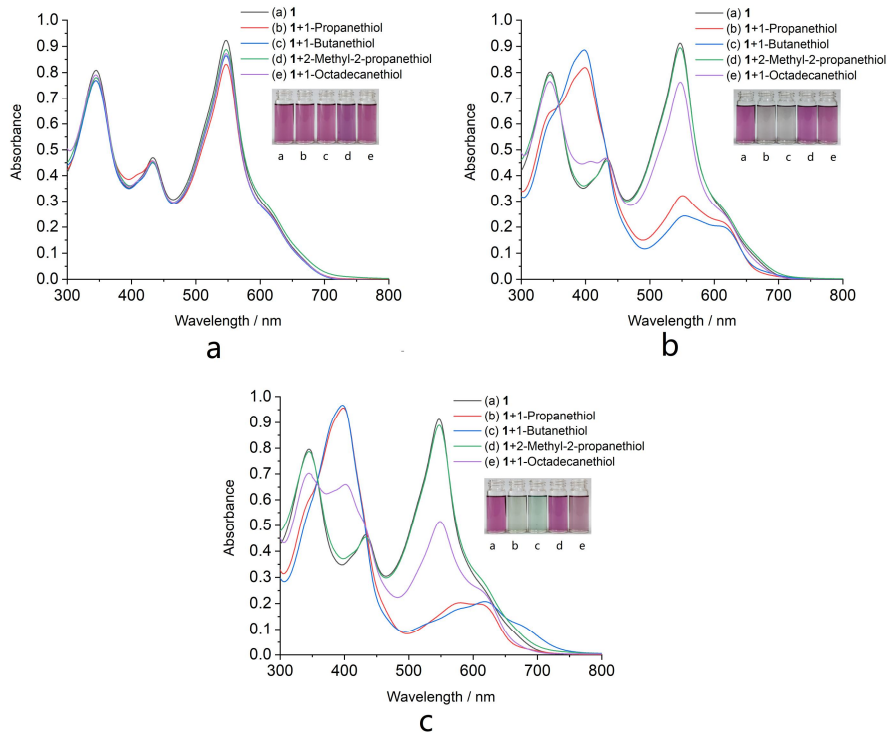

Figure S22. UV-Vis absorption spectra and photos of **1** in chloroform upon the addition of an aliphatic thiol. (a): Immediately after the addition and after (b): 6 h; (c): 12 h.

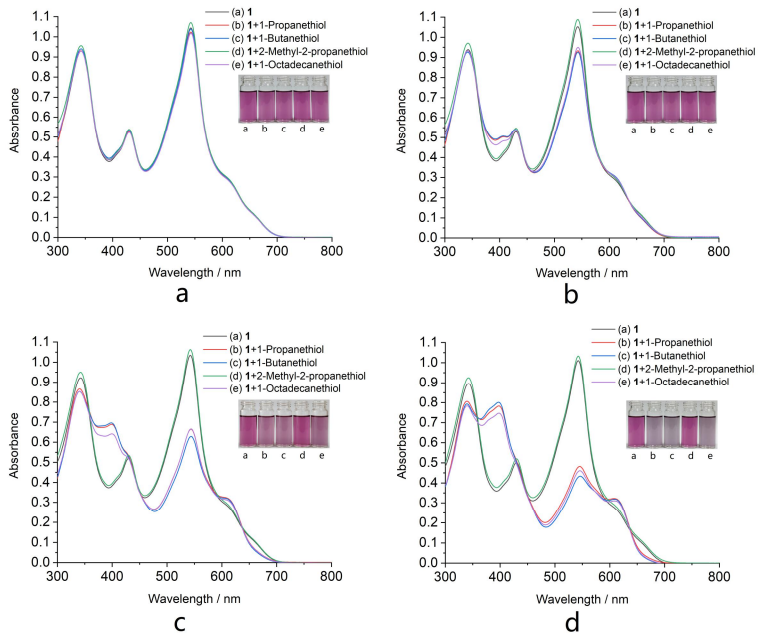

Figure S23. UV-Vis absorption spectra and photos of **1** in THF upon the addition of an aliphatic thiol. (a): right after the addition and after (b): 6 h; (c): 12 h; (d): 20 h.

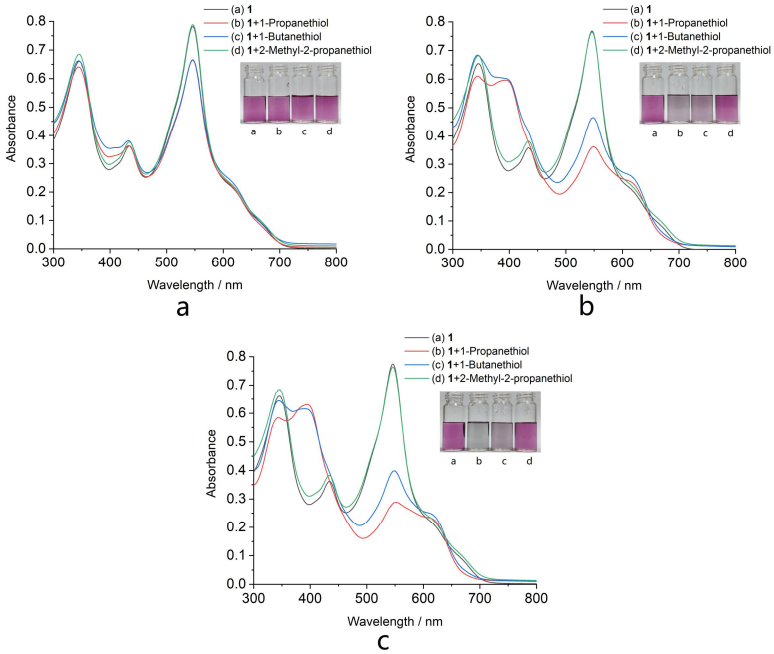

Figure S24. UV-Vis absorption spectra and photos of **1** in DMSO upon the addition of an aliphatic thiol. (a): right after the addition and after (b): 6 h; (c): 12 h.

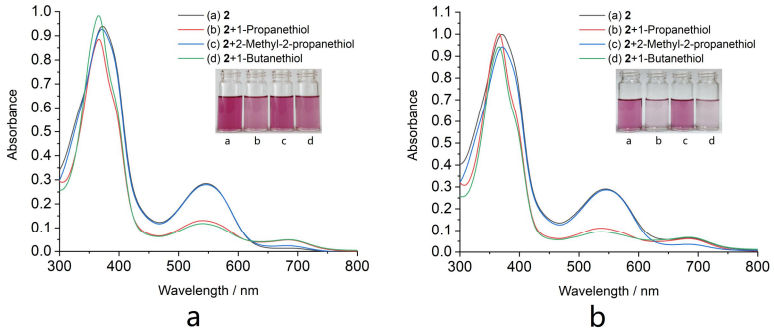

Figure S25. UV-Vis absorption spectra and photos of **2** in chloroform upon the addition of an aliphatic thiol. (a): right after the addition and after (b): 2 h.

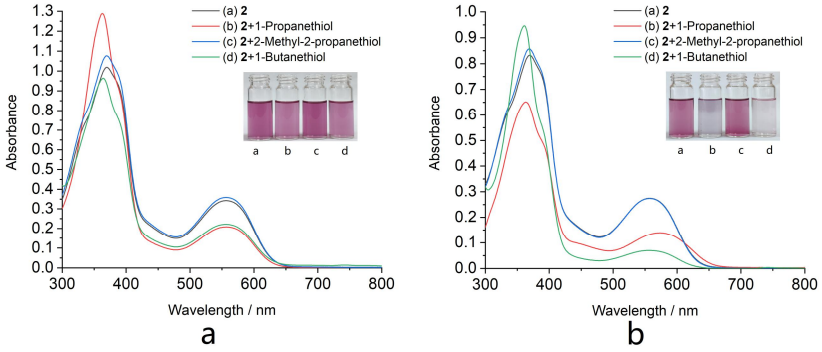

Figure S26. UV-Vis absorption spectra and photos of **2** in THF upon the addition of an aliphatic thiol. (a): right after the addition and after (b): 6 h.

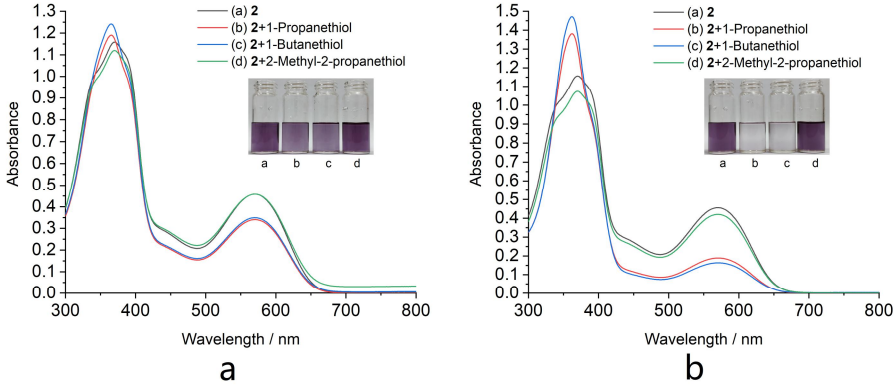

Figure S27. UV-Vis absorption spectra and photos of **2** in DMSO upon the addition of an aliphatic thiol. (a): right after the addition and after (b): 4 h.

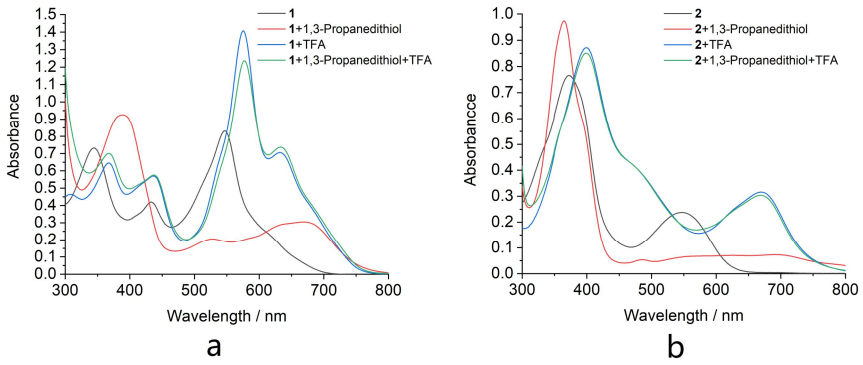

Figure S28. UV-Vis spectra of **1** (a) and **2** (b) before and after being treated with 1,3-propanedithiol, TFA, or both in $CHCl_3$.

Ⅳ. X-ray Experimental

Crystal data for **1**: A flake crystal of formula ($C_{81}H_{84}N_{12}$)·3.6($CHCl_3$), having approximate dimensions: 0.12 mm x 0.003 mm x 0.002 mm, was used for the X-ray crystallographic analysis. The X-ray intensity data were measured using a Bruker SAINT diffractometer.

The frames were integrated with the Bruker SAINT software package using a narrow-frame algorithm. The integration of the data using a monoclinic unit cell yielded a total of 89206 reflections, of which 15960 were independent (completeness = 99.4 %%, R_{int} = 5.53%). Details of crystal data, data collection and structure refinement are listed in Table S1.

For compound **1** all the non-hydrogen atoms were refined anisotropically. Carbon bound H-atoms were located at the geometrical positions whereas H-atoms bonded to nitrogen were found from the difference Fourier maps with two constraints of N–H = 0.86(1) Å and thermal parameters of $U_{iso}(H) = 1.2U_{eq}(N)$. During the refinement, several separate large residual peaks (within 1.08–6.54 e·Å^3) were found crystallographically to be situated near the host molecule. According to their linkage connectivity, they were inferred to be chloroform molecules. However, some tentative refinements did not give a satisfactory outcome because of serious disorder. So the contribution of these putative solvent molecules to the diffraction pattern was subtracted using the SQUEEZE procedure of PLATON. The result indicated that the solvent-accessible void in the unit cell has a volume of 510.2 Å^3 (consisting of about 6.05% of the crystal volume, equally distributed across two cavities at asymmetric units of (0.000 0.000 0.500) and (0.500 0.500 0.000), respectively). The residual electron density count amounted to approximate 148 e per unit cell, corresponding to nearly 2.552 molecules of $CHCl_3$. Therefore, every molecule of compound **1** was considered to be associated with 0.6 additional chloroform molecule due to z = 4, meaning the practical formula should be ($C_{81}H_{84}N_{12}$)·3.6($CHCl_3$).

Compound **1** as a whole adopts a twisted chair-like conformation in the solid state. The observed conformation has three intramolecular N-H···N hydrogen bonds with the N···N distances being in the range of 2.626(3) to 2.862(3) Å.

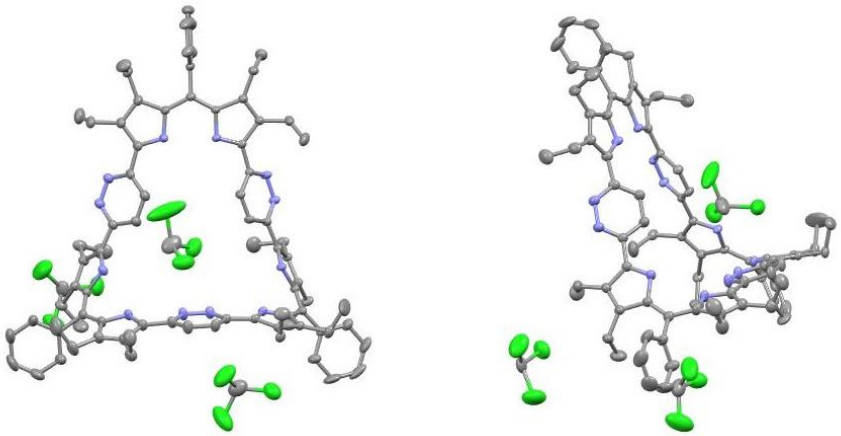

Figure S29. Views of the single crystal structure of compound **1**.

Table S3. Crystal data for 1.

Empirical Formula		$(C_{81}H_{84}N_{12})\cdot 3.6(CHCl_3)$
Formula Weight		1583.70
Temperature		170.15 K
Crystal Colour, Habit		Dark purple, flake
Crystal Dimensions		0.12 x 0.03 x 0.02 mm^3
Crystal System		Monoclinic
Space Group		P 1 21/n 1
Lattice Parameters	*a*/Å	11.8725(2) Å
	b/Å	16.7463(3) Å
	c/Å	42.5496(8) Å
	α/deg	90°
	β/deg	94.8920(10)°
	□/deg	90°
	V/$Å^3$	8428.9(3) $Å^3$
Z Value		4
F_{000}		3312
No. of Reflections Measure	Total:	89206
	Unique:	15960 [R(int) = 0.0553]

R1; *wR2* (refined on F^2, all data)	0.0895, 0.2260
Goodness of Fit Indicator (GOF)	1.037
R1; *wR2* (refined on F, I>2σ(*I*))	0.0768, 0.2152
CCDC number	2031025

Ⅴ. Mass Spectrometric Studies

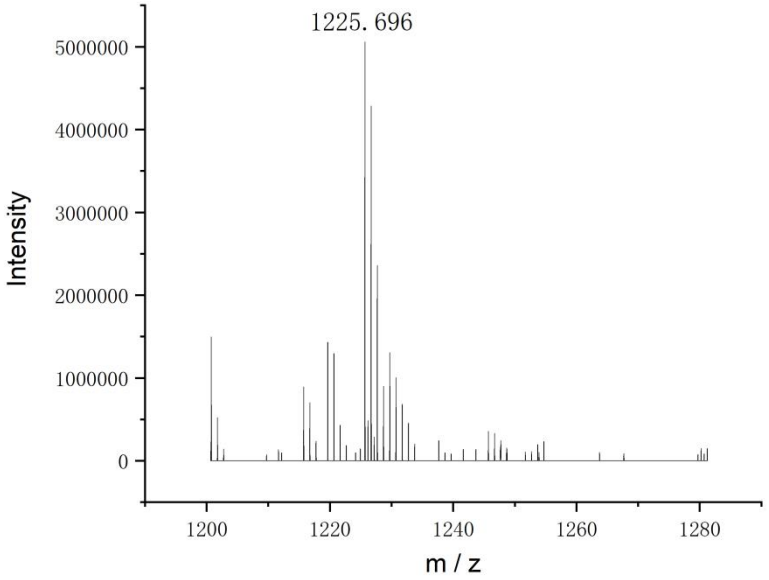

Figure S30. MALDI-TOF high resolution mass spectrum of **1**.

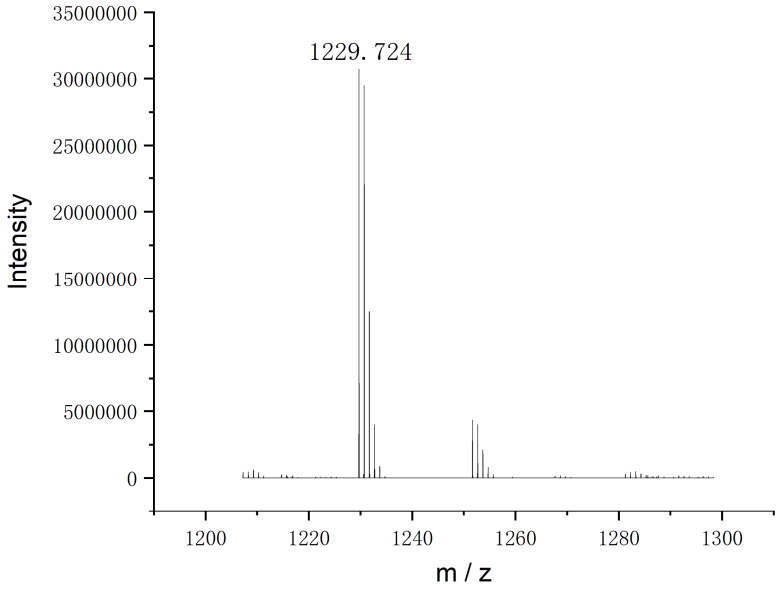

Figure S31. MALDI-TOF high resolution mass spectrum of **2**.

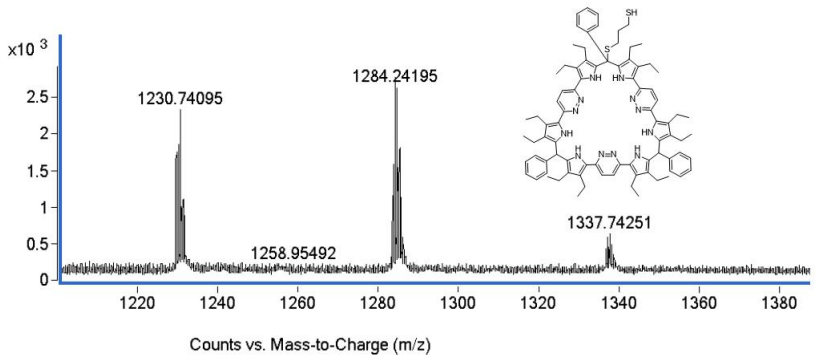

Figure S32. Q-TOF high resolution mass spectrum of the reaction mixture of **2** and 1,3-propanedithiol. Calcd for $C_{84}H_{97}N_{12}S_2$: 1337.74006. Found: 1337.74251.

VI. HPLC Analysis

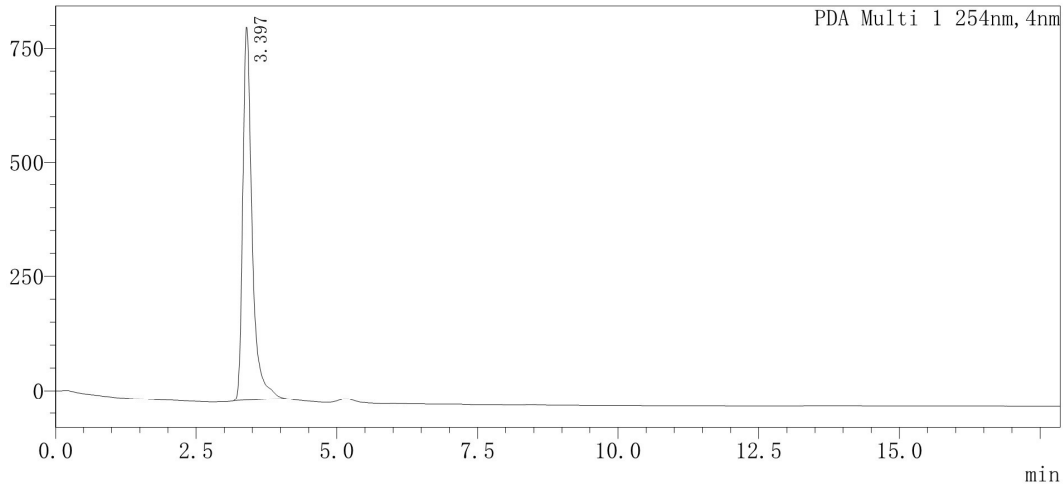

PDA Ch1 254nm

	RT(min)	Area	Height	Area(%)	Height(%)
1	3.397	9464262	817197	100.000	100.000

Figure S33. The HPLC chromatogram of **2**. A mixture of n-hexane and 2-propanol (30 : 70, v : v) was used as the eluent.

Ⅶ. Calculations

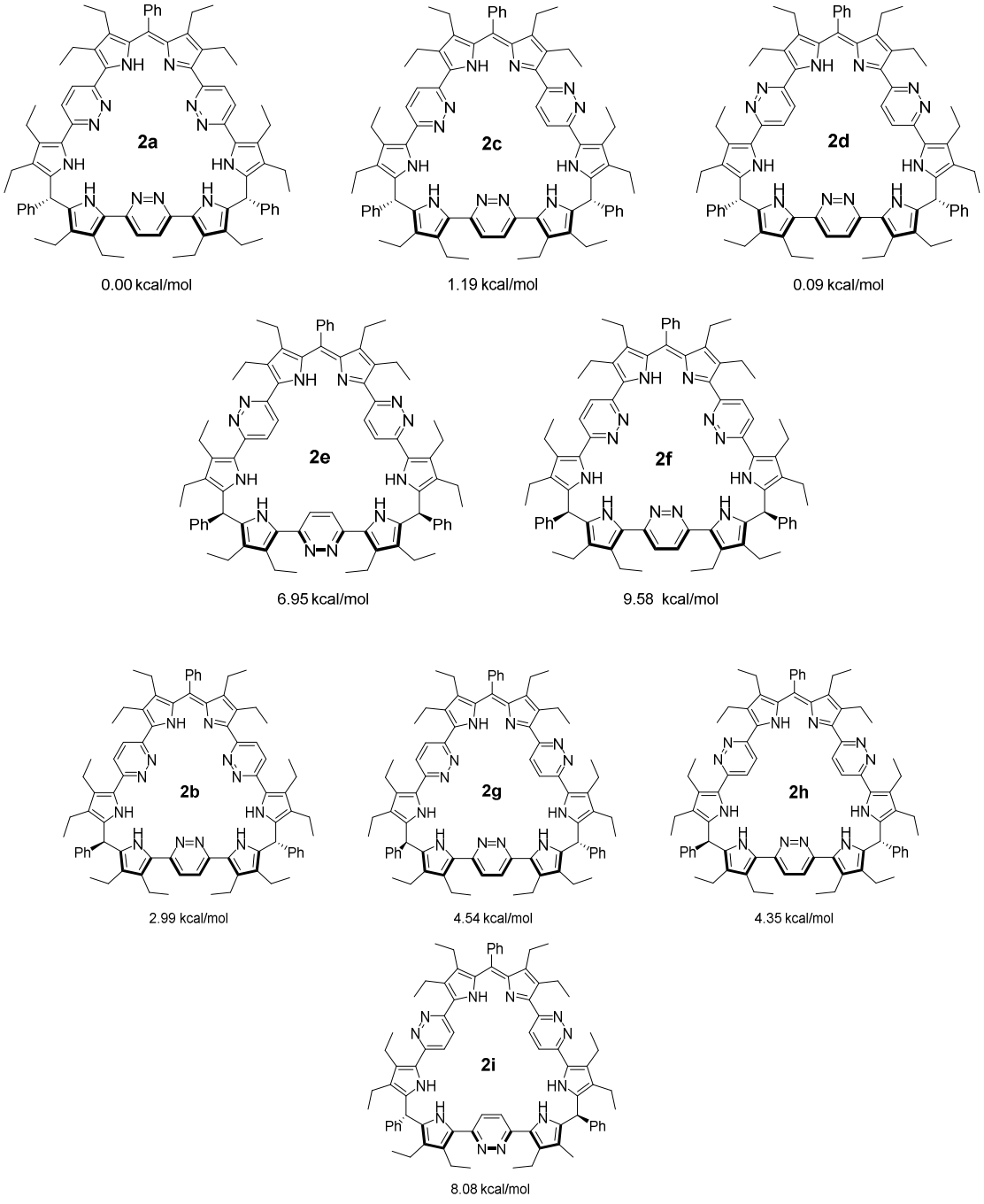

Figure S34. Relative energies (kcal/mol, reference to compound **2a**) for various isomers of compound **2**. These energies were obtained at the B3LYP/6-31G(d,p)//B3LYP/6-31G(d,p) level of theory.[2] The geometries of the various putative structures were fully optimized without symmetry assumptions using Becke's three-parameter hybrid functional combined with the Lee–Yang–Parr correlation functional (B3LYP) along with 6-31G(d,p) basis set.

Ⅷ. Supporting References

1. Zhang, X.; Zhang, Z.; Lei, C. *Faming Zhuanli Shenqing* 2019, CN109956934 A 20190702.
2. Setsune, J.-i.; Toda, M.; Watanabe, K.; Panda, P. K.; Yoshida, T., *Tetrahedron Letters* 2006**, 47**, 7541-7544.
3. Gaussian 09, Revision E.01, Frisch, M. J.; Trucks, G. W.; Schlegel, H. B.; Scuseria, G. E.; Robb, M. A.; Cheeseman, J. R.; Scalmani, G.; Barone, V.; Mennucci, B.; Petersson, G. A.; Nakatsuji, H.; Caricato, M.; Li, X.; Hratchian, H. P.; Izmaylov, A. F.; Bloino, J.; Zheng, G.; Sonnenberg, J. L.; Hada, M.; Ehara, M.; Toyota, K.; Fukuda, R.; Hasegawa, J.; Ishida, M.; Nakajima, T.; Honda, Y.; Kitao, O.; Nakai, H.; Vreven, T.; Montgomery, J. A., Jr.; Peralta, J. E.; Ogliaro, F.; Bearpark, M.; Heyd, J. J.; Brothers, E.; Kudin, K. N.; Staroverov, V. N.; Kobayashi, R.; Normand, J.; Raghavachari, K.; Rendell, A.; Burant, J. C.; Iyengar, S. S.; Tomasi, J.; Cossi, M.; Rega, N.; Millam, J. M.; Klene, M.; Knox, J. E.; Cross, J. B.; Bakken, V.; Adamo, C.; Jaramillo, J.; Gomperts, R.; Stratmann, R. E.; Yazyev, O.; Austin, A. J.; Cammi, R.; Pomelli, C.; Ochterski, J. W.; Martin, R. L.; Morokuma, K.; Zakrzewski, V. G.; Voth, G. A.; Salvador, P.; Dannenberg, J. J.; Dapprich, S.; Daniels, A. D.; Farkas, Ö.; Foresman, J. B.; Ortiz, J. V.; Cioslowski, J.; Fox, D. J. Gaussian, Inc., Wallingford CT, 2009.